Enhanced Visualization of Late-Stage Transitional Structures using Vortex Identification and Automatic Feature Extraction

Kai Müller, Ulrich Rist, and Siegfried Wagner [1]

Abstract. The unsteady Navier–Stokes equations offer a large variety of instantaneous solutions even for rather simple boundary conditions once the relevant spatial and temporal scales of the problem at hand are adequately resolved. This is especially true for DNS (Direct Numerical Simulation) of laminar-turbulent transition, where an initially laminar flow, disturbed by some unsteady fluctuations "breaks down" into small-scale high-frequency turbulence. When trying to study and understand this process, one faces the problem of identifying the relevant structures to describe the flow which consist of vortices and shear layers, and on their isolation for further investigation. Here, we present a post-processing method based on the vortex definition proposed by Jeong & Hussain [5] and on Feature Extraction similar to Silver [13] that allows to successfully identify, isolate and track vortical features in a transitional boundary layer.

1 INTRODUCTION

Apparently, vortices appear in almost every flow from the small-scale turbulent eddies responsible for energy dissipation to the large-scale motions in a planet's atmosphere. Thus, it is quite obvious that researchers seeking for a description or a deeper understanding of a certain flow problem usually look for a concept that relies on a description of the flow field in terms of induced velocity, vorticity, pressure, etc. based on previously identified vortices.

However, the proper identification of a vortex is a difficult problem, especially when dealing with digital data on a computer. Firstly, because of the dependence of the observed flow field (in terms of streamlines or particle traces) on the frame of reference of the observation. Secondly, even when using criteria which are Galilean invariant, there is much controversy on how to define a vortex. Recently, different methods have been compared by Banks & Singer [1] and Jeong & Hussain [5], for instance.

Mathematically, the most rigorous method is perhaps the eigenvalue criterion described by Chong *et al.* [2] which identifies regions of complex eigenvalues of the velocity-gradient tensor which are connected to a possible occurrence of spiraling or closed streamlines in some frame of reference. However, researchers working with this condition find it difficult to interpret, mainly because of jitter produced by numerical noise. In addition, Jeong & Hussain [5] show examples where this method is not appropriate, i.e., not every region that exhibits 'swirl' in some frame of reference moving with the flow consists of a vortex. Their own criterion, repeated here in §3, does not exhibit these problems. Because this criterion captures the pressure minima in planes perpendicular to the vortex axis, it is phenomenologically equivalent to the definition used by Banks & Singer [1] for their predictor-corrector scheme. Nevertheless, we preferred to implement the method of Jeong & Hussain since it is much easier to program than the method of Banks &

[1] Institut für Aerodynamik und Gasdynamik der Universität Stuttgart, Pfaffenwaldring 21, 70550 Stuttgart, Germany

ECCOMAS 98.
Published in 1998 by John Wiley & Sons, Ltd.

Singer. In addition, the first method automatically gives reasonable information about the extent and hence the shape of the identified vortices.

The next aspect that must be addressed here is the enormous amount of numerical data reduction that is possible using feature-based visualization techniques, as proposed for instance by Samtaney *et al.* [12], Silver [13], or Silver & Wang [14]. Mainly, their technique consists of *identification*, *segmentation*, and *tracking* of features based on thresholds of the vorticity magnitude. The first subtask is connected with the vortex-identification problem described above, the second simply means a decomposition of a given data set into the features it contains, while tracking seems only necessary when dealing with unsteady data, in order to answer questions about 'birth', evolution or 'death' of structures. At present, such techniques are not yet widely used, nor are parts thereof already implemented into standard visualization-software systems. However, our examples show that some data pre-processing routines are sufficient to implement the present ideas and that any standard visualization system can be used to visualize the resulting time-dependent three-dimensional scalars.

We have combined the method of Jeong & Hussain for vortex identification with feature extraction and tracking after Silver *et al.* into one or two algorithms and we want to demonstrate their usefulness here for a practical application. For the latter we have chosen the DNS of laminar-turbulent transition of a flat-plate boundary-layer because of our year-long experience in that field [15]. At present we are testing the applicability of the methods for other numerical simulations as well. The advantage of transitional flow fields, however, is that vortices of different size and strength as well as increasing complexity appear as the laminar flow breaks down into random, small-scale turbulent motion. Another challenge is the simultaneous presence of high-shear layers and vortices which cannot be distinguished using vorticity as in Silver *et al.*, for instance.

2 TRANSITIONAL FLOW FIELD

Our concern here is the identification and extraction of late-stage vortical structures in our DNS of K-type transition experiments performed by Kachanov *et al.* in Novosibirsk, Russia (cf. Kachanov [7]). As shown earlier in Rist & Fasel [10] or Rist & Kachanov [11], our simulations are in excellent agreement with the experimental data and hence provide additional insight into the flow-field because of the simultaneous acquisition of all velocity components which was not possible in the experiment, so far.

Here, a simulation has been performed using 65 spectral modes in z-direction on a $x \times y$-grid with 190,000 nodes. The number of unknowns at each time instant thus amounts to $74 \cdot 10^6$ and, starting from an initially laminar flow, $\approx$7,000 time steps have been computed in order to capture the small-scale unsteady motions.

Time-wise periodic disturbances have been introduced into the boundary-layer flow along a flat plate at $x = 250$mm from the leading edge. After amplification and nonlinear interactions between 2D and 3D waves, the first so-called spikes appear in hot-wire velocity signals at $x = 400$mm as a typical indication for imminent laminar-turbulent transition. Further downstream, at $x \approx 500$mm, the flow is already turbulent.

From experimental flow visualizations it is already known that Λ-shaped vortices appear and somehow shed smaller vortices in the transitional region situated here between $x \approx 400$mm and $x \approx 500$mm. An instantaneous view of the first such event, i.e., a Λ-vortex and a 'hairpin'-shaped vortex at its downstream tip, is shown in Fig. 1 by applying the vortex criterion described in §3. The indicated cuts will be used for verification of the method further down.

According to the unsteady nature of the physical problem, the relative time (or phase ϑ) is im-

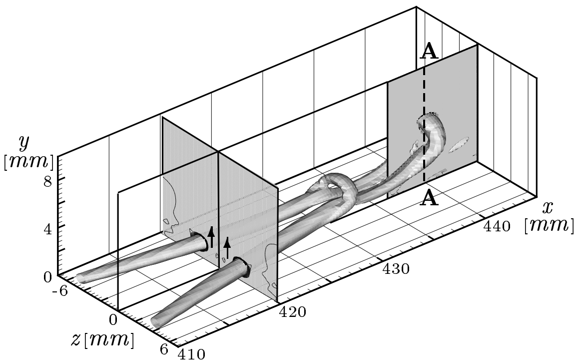

Figure 1. View of flow-field structures at $\vartheta = 1/6$ using $\lambda_2 < 0$ and an illustration of cuts used for verification. Arrows at $x = 420$mm indicate sense of rotation.

portant here. It is defined relative to the period of forcing at $x = 250$mm as a fraction of that period. The vortices rotate in the direction indicated by the two arrows in the cutting plane at $x = 420$mm and move low-speed fluid away from the wall. This leads to a region of instantaneous streamwise velocity defect between the 'legs' of the Λ and especially at the tips of the loops where the vortex-induced velocity points upstream. Thus, when a hot-wire anemometer is placed in such a region it will indicate a 'spike' every time a vortex passes by.

3 VORTEX IDENTIFICATION

As already mentioned, we want to use the method proposed by Jeong & Hussain [5] for vortex identification. So far, only a few examples for its use have appeared in the literature, like for instance, Wintergerste *et al.* [16], Cui *et al.* [3], Jeong *et al.* [6], or our own work [9].

Let $\nabla \mathbf{u}$ be the velocity-gradient tensor of an incompressible fluid and $u_{i,j}$ its components, where the first index indicates the i^{th} component of the velocity vector and the second differentiation with respect to the j^{th} direction. Then

$$\mathbf{S}_{ij} = \frac{1}{2}(u_{i,j} + u_{j,i}) \ , \quad \text{and} \quad \mathbf{\Omega}_{ij} = \frac{1}{2}(u_{i,j} - u_{j,i})$$

are the symmetric and antisymmetric parts of $\nabla \mathbf{u}$, respectively. If viscous effects and unsteady irrotational straining are neglected, the tensor (1)

$$\underbrace{\mathbf{S}_{ij}^2 + \mathbf{\Omega}_{ij}^2}_{(1)} = -\frac{1}{\rho} p_{,ij}$$

is connected to the Hessian of the pressure, $p_{,ij}$, i.e., the matrix of the second spatial derivatives of p in 3D space. Thus, if the pressure has a local minimum, its Hessian must be positive definite. This is equivalent to a negative definite matrix $\mathbf{S}_{ij}^2 + \mathbf{\Omega}_{ij}^2$, and hence, in a planar cut, a local pressure minimum will exist if there is a negative definite submatrix in (1). This condition is met when two negative eigenvalues occur. Therefore, if we order the eigenvalues of (1)

$$\lambda_1 \geq \lambda_2 \geq \lambda_3 \ ,$$

$\lambda_2 < 0$ will mean two negative eigenvalues, and hence a local pressure minimum in some cutting plane through the pressure field belonging to rotation. The criterion $\lambda_2 = 0$ bounds such minima at

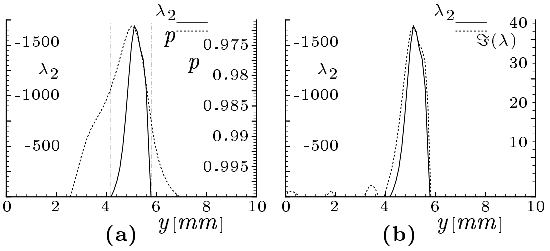

Figure 2. Comparison of the second largest eigenvalue λ_2 of the matrices in eqn. (1) with the pressure (a) and the imaginary parts of the eigenvalues of $\nabla \mathbf{u}$ (b) along cut **A - - A** ($x = 440$mm, $z = 0$) in Fig. 1.

the inflection points when cutting through the minimum. This can be seen in Fig. 2 in a comparison of λ_2 with pressure and the criterion of Chong *et al.* [2] on a line (**A - - A**) that cuts right through the hairpin vortex in Fig. 1. Clearly, $\lambda_2 = 0$ (emphasized by the vertical dash-dotted lines) correlates very well with inflection points in the pressure which occur at different levels of p. Cutting p at a specific threshold will certainly give a different picture and choosing an appropriate threshold value is a difficult task if one considers that pressure is influenced by other events apart from swirling motion. Therefore, $\lambda_2 < 0$ is much easier to use than pressure especially for iso-surface generation in 3D because of the steep gradients around $\lambda_2 = 0$ which make the results less dependent on the proper choice of the threshold. In addition, stronger vortices yield a stronger gradient and also a much lower λ_2 than weaker ones. Thus, weaker vortices may be removed from the visualization by a low threshold.

Compared to the criterion based on complex eigenvalues of $\nabla \mathbf{u}$ [2], the $\lambda_2 < 0$ - criterion is never in contradiction to Chong *et al.* [2]. In addition, it is more 'conservative', i.e., it always remains below the curve for $\Im(\lambda)$ and does not produce small side peaks at other y. Thus, it will cause less jitter when used in 3D than the complex eigenvalue criterion.

Cuts through the legs of the Λ-vortex at $x = 420$mm in Fig. 3 exhibit two local structures connected with the presence of the vortex: low pressure to balance the centrifugal forces of the swirling motion in Fig. 3a) and maxima of the in-plane vorticity $|\omega_x|$ as an indication of rotation in Fig. 3b). Still, the vorticity depicts regions of spanwise shear also, especially close to $y = 0$ because of the no-slip boundary condition at the wall. Since the spanwise

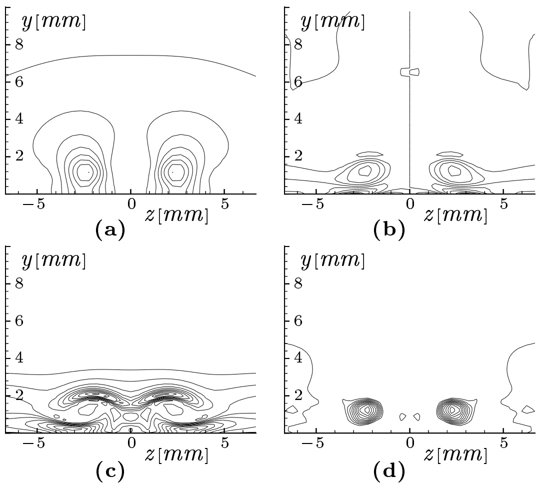

Figure 3. Comparison of pressure (a), x-component of vorticity (b), vorticity magnitude (c), and $\lambda_2 < 0$ (d) at $x = 420$mm, $\vartheta = 1/6$.

shear dominates over all other shear components within the boundary layer, vorticity magnitude in Fig. 3c) is totally unable to detect the vortex here. Instead of a maximum there is nearly a minimum at the position of the vortex. Here, the clearest picture of the cuts through the vortex' legs is given by contours of $\lambda_2 < 0$. However, once the vortex is identified based on $\lambda_2 < 0$, the shear layers in the vorticity plots are identified as well.

Longitudinal cuts of the vorticity magnitude in

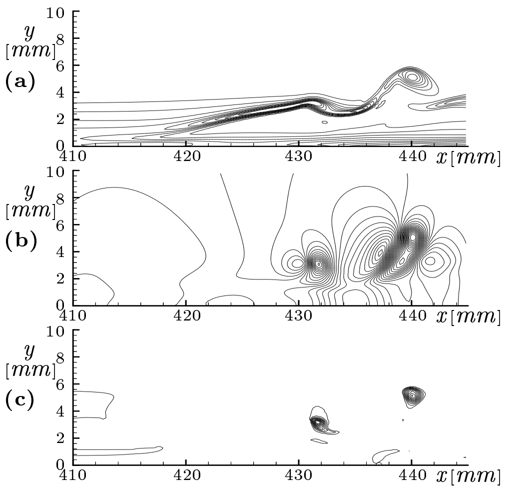

Figure 4. Comparison of vorticity magnitude (a), pressure (b), and $\lambda_2 < 0$ (c) at $z = 0$, $\vartheta = 1/6$.

Fig. 4 a) also cannot distinguish between high-shear layers and rotation, despite the fact that the Λ-vortex and the hairpin vortex are cut at their downstream ends lying near the outer edge of the boundary layer where less surrounding shear exists. The pressure field in Fig. 4 b) is governed by a sequence of minima and maxima together with wall effects and a superimposed large-scale variation, and hence does not yield a clear picture either. Therefore, the need for a vortex criterion, like $\lambda_2 < 0$ which apparently works very well in Fig. 4 c).

The unsteady nature of the structures $\lambda_2 < 0$ is best illustrated in Fig. 5. An increasing number of hairpin vortices (I – V) appears as time evolves. The first of these develops into a nearly perfect ring with two long tails extending down towards the wall while the others turn into similar, Ω-like loops. The loops travel much faster than the Λ-vortex and eventually snatch away from the 'body' of the Λ as

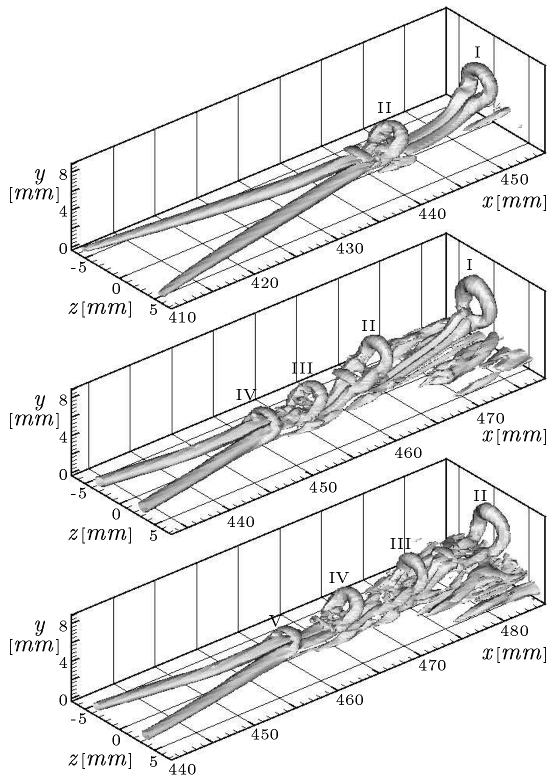

Figure 5. Iso-surfaces $\lambda_2 = -200$ for three time instants, $\vartheta = 0.335$, 0.605, and 0.845, from top to bottom, respectively.

a new hairpin vortex whose tails move towards the wall. In the meantime, the next loop has already started to form as a small 'bridge' between the legs of the Λ-vortex.

The rather 'clean' shape of the first hairpin might be due to the fact that this one evolves into a rather undisturbed flow, while the others might interact with each others. The generation of new structures beside $z = 0$ could also be caused by such interactions, but this has to be clarified in further investigations. As more and more vortices/structures evolve, the picture and possible interactions get increasingly complex. This is why we needed a tool for feature extraction and their tracking.

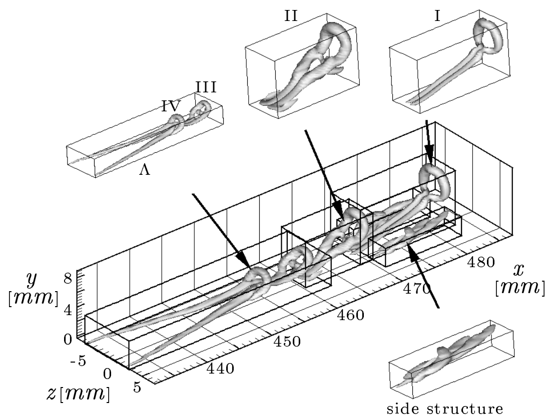

Figure 6. Late-stage vortices at $\vartheta = 2/3$ together with extracted individual structures in their bounding boxes.

4 FEATURE EXTRACTION AND TRACKING

Once the structures have been found, it might be necessary to identify, separate and track them, especially for unsteady flows as in our case (c.f., the numbering in Fig. 5). This is not only important to reveal details which are hidden by certain structures in a data set (depending on the view direction), but also as a first step towards understanding the interaction between different structures. For this we use "region growing" [14] starting at the λ_2-minimum of the data set. All the points surrounding this seed point in x, y, and z direction are considered until $\lambda_2 > 0$ is encountered. During traversal of the data all points with $\lambda_2 \leq 0$ plus one surrounding 'shell' of positive values are copied to a temporary array whilst the data points in the original array and belonging to the current vortex are set to some large positive constant. This removes regions which have already been traversed from reconsideration and allows to start the extraction for the next vortex automatically at the new λ_2-minimum. Thus, a list of vortices ordered by their strength is generated. Simultaneously to λ_2 other data belonging to the vortex (p or ω, for instance) can be extracted from the flow, as well. However, it should be noted here that the separation of one structure into two or more which we observe is dependent on the threshold value for $\lambda_2 < 0$ used for visualization. When two vortices are stretched apart, the region between them gets weaker and weaker and therefore it seems acceptable to cut them into two for further investigations (of the large-amplitude structures).

In order to reduce the resulting data, only those within a bounding box fitted around the identified structure are stored and processed further, cf. Fig. 6. Thus, the original amount of data is reduced despite some duplication of information in the overlap regions of the bounding boxes belonging to neighboring vortices.

Once the vortices have been extracted, they can be shown isolated or in connection as illustrated in Fig. 6. Each vortex can be given a tag, an individual color, etc., as has already been demonstrated by Silver, Zabusky *et al.*

For animation and tracking, the list of extracted vortices is traversed again and rearranged. A data structure is built up during re-traversal of the list that identifies corresponding vortices or parts thereof by an overlapping criterion when comparing data of two consecutive time steps. Thus, the development of individual structures can be tracked and analyzed over time depending on the needs of the researcher.

5 CONCLUSIONS

It has been shown that identification and extraction of vortices in a transitional flow field is an important first step towards a more abstract visualization and understanding of the flow field extracted from numerical data. The criterion proposed by Jeong & Hussain has been verified and apparently works very well in our case.

We are well aware of some scepticism against using this method [4]. However, we could not identify a problem yet. For instance, the observation by

Lugt & Copeland [8] that not every vortex produces a local pressure minimum holds only for vortices with a Reynolds number around 10. This would mean a vortex diameter of $15 \cdot 10^{-3}$mm in our case which is really far away from the size of the structures we wanted to observe. Anyway, structures of that size are well below the step size of the grid in the present simulation. In addition, it has been confirmed that complex eigenvalues of the velocity-gradient tensor as a necessary condition for $\lambda_2 < 0$ is not violated.

Choosing a threshold other than $\lambda_2 = 0$ is rather save because of the steep gradients of λ_2 at the border of strong vortices. Vortices of different strength of rotation can be distinguished by their λ_2 minimum and weak vortices may be removed by choosing a lower threshold. Thus, our extraction algorithm based on λ_2 automatically extracts the strongest vortices first before it continues with the weaker ones. This leads to a hierarchical list of structures for further processing.

We believe that the techniques described here will provide a valuable tool to gain deeper insight into complicated unsteady flow phenomena. Therefore, its applicability to other flows is currently under investigation, as well.

REFERENCES

[1] D.C. Banks and B.A. Singer, 'Vortex tubes in turbulent flows: Identification, representation, reconstruction', in *Visualization '94, Oct. 17–21, 1994, Washington, D.C.*, eds., R.D. Bergeron and A.E. Kaufman, pp. 132–139, Los Alamitos, CA, (1994). IEEE CS-Press. Also as ICASE Report 94-22.

[2] M.S. Chong, A.E. Perry, and B.J. Cantwell, 'A general classification of three-dimensional flow fields', *Phys. Fluids A*, **2 (5)**, 765–777, (1990).

[3] Y. Cui, B. Tanguay, A. Bottaro, and P.A. Monkewitz, 'Spatial numerical simulations and experiments on the breakdown of streamwise vortices in a Blasius boundary layer', in *Advances in Turbulence VI*, eds., S. Gavrilakis et al., pp. 325–328. Kluwer Academic Publishers, (1996).

[4] U. Dallmann. Personal communication, 1997.

[5] J. Jeong and F. Hussain, 'On the identification of a vortex', *J. Fluid Mech.*, **285**, 69–94, (1995).

[6] J. Jeong, F. Hussain, W. Schoppa, and J. Kim, 'Coherent structures near the wall in a turbulent channel flow', *J. Fluid Mech.*, **332**, 185–214, (1997).

[7] Yu.S. Kachanov, 'Physical mechanisms of laminar-turbulent boundary-layer transition', *Ann. Rev. Fluid Mech.*, **26**, 411–482, (1994).

[8] H.J. Lugt and G.S. Copeland, 'On pressure minima in two-dimensional vortex flows', *Phys. Fluids*, **6 (6)**, 2230–2232, (1994).

[9] D. Meyer, U. Rist, and S. Wagner, 'DNS of the generation of secondary Λ-vortices in a transitional boundary layer', in 7^{th} *European Turbulence Conference, Saint Jean Cap Ferrat, France, June 30 – July 3, 1998*, ed., U. Frisch, (1998).

[10] U. Rist and H. Fasel, 'Direct numerical simulation of controlled transition in a flat-plate boundary layer', *J. Fluid Mech.*, **298**, 211–248, (1995).

[11] U. Rist and Yu.S. Kachanov, 'Numerical and experimental investigation of the K-regime of boundary-layer transition', in *Laminar-Turbulent Transition, Proc. IUTAM Symp. Sendai, Japan, 1994*, ed., R. Kobayashi, pp. 405–412, Berlin, (1995). Springer-Verlag.

[12] R. Samtaney, D. Silver, N. Zabusky, and Cao J., 'Visualizing features and tracking their evolution', *Computer*, **27 (7)**, 20–27, (1994).

[13] D. Silver, 'Object-oriented visualization', *IEEE Computer Graphics and Applications*, **15 (3)**, 54–62, (1995).

[14] D. Silver and X. Wang, 'Tracking and visualizing turbulent 3D features', *IEEE Transactions on Visualization and Computer Graphics*, **3 (2)**, 129–141, (1997).

[15] S. Wagner, 'Direct numerical simulation of laminar-turbulent transition', in *Computational Methods in Applied Sciences '96*, eds., J.-A. Désidéri, C. Hirsch, P. Le Tallec, M. Pandolfi, and J. Périaux, pp. 77–90, Chichester, (1996). John Wiley & Sons.

[16] T. Wintergerste and L. Kleiser, 'Direct numerical simulation of transition in a three-dimensional boundary layer', in *Transitional boundary layers in aeronautics*, eds., R.A.W.M. Henkes and J.L. van Ingen, pp. 145–153, Amsterdam, (1996). North-Holland.